

Continuous Wave RF Gun: Computer Simulation, Design and Tuning.

A.Alimov, O.Chubarov, D.Ermakov, B.Ishkhanov, I.Piskarev, A.Tiunov, V.Shvedunov, V.Yaliyan

Institute of Nuclear Physics, Moscow State University, Moscow, 119899, Russia

Abstract

The results of computer simulation, design, cold measurements and tuning of continuous wave RF gun are presented. RF gun consists of 12 accelerating and 11 coupling cells of standing wave on-axis coupled structure with the tungsten impregnated cathode inserted into the first cell. Cells lengths and shunt impedances are optimized in order to reach high capture efficiency with the low values of electric field strength in CW regime. RF gun is capable to supply 34kW/0.5MeV electron beam with 53 kW, 2450 MHz CW klystron.

INTRODUCTION

Experience obtained during the construction of Moscow RTM and equipment developed in the framework of the RTM project [1] were used for a design of high power CW linac with RF gun. The main problem of cw accelerator structures is the high levels of RF power dissipated per structure unit length. Because of this, gap voltages are about 10 times less, than those in pulsed linacs.

1. COMPUTER SIMULATION.

A simulation procedure included optimisation of the geometry of accelerator structures and calculations of the beam dynamics by means of the method of consequent approximations. Methods for optimisation the pulsed RF gun were published elsewhere[2]. Our CW linac with RF gun is to be used with the RF equipment, based on a 22 kW CW klystron with operating frequency 2450 MHz, designed for the Moscow RTM project. The accelerating field of the linac was limited by following conditions: RF power, dissipated in the linac must be less than 17 kW - limit of thermo-elastic deformations defines maximum RF power, dissipated in the accelerating cell, by the value 3kW, corresponding gap voltage is 35-70 kV.

Optimisation of the geometry and the choice of parameters for the first three cells must be done very thoroughly, because bunch forming takes place in it. For the computer simulation we used such programs as PRUD0[3], RTMTRACE [4] and PARMELA[5].

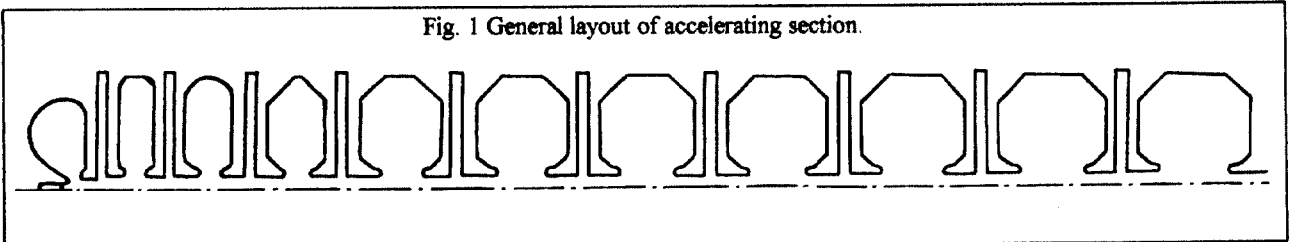
1.1 Geometry optimisation.

Preliminary calculations showed that only electrons, emitted from the cathode beginning with the moment of increasing the accelerating field (zero phase) in the first cell, where the cathode was inserted, to the moment when the phase was 70 degrees, took part in forming the output beam of the accelerator. Hence, in calculations we took into account only a beam with 70 degrees phase length. Fig 2 shows the dependence of the minimum and maximum energy of the particles in the bunch, emitted in the phase range 0-70 degrees, on the gap length of the first cell at the gap voltage value of 35 kV. Figure also shows the relative values of RF power, dissipated in the cell. Same dependences have been obtained for the different values of gap voltages. The optimal value of the gap length, obtained from the calculations was 5 mm. Gap voltage was equal to 55 kV. This value was chosen as an optimal. In order to increase the quality and shunt impedance, the first accelerator cell was made nonsymmetrical. The choice of cathode position was carried out by calculating the beam dynamics in the first cell. The longitudinal dimensions of the second and third cells are determined by following factors: energy gain, phase correlations at the entrance of the next cell, allowed level of RF power dissipated in the cell. The transverse diameters are determined by the requirement of providing the resonant frequency 2450 MHz (taking into account the presence of coupling slots). Calculations of the parameters of other cells and of beam dynamics in the linac were carried out in conventional way [6]. General layout of the linac with the RF gun and the distribution of the accelerating field on the axis are presented in Fig 1 and Fig 3, respectively.

1.2. Beam characteristics.

As mentioned above, the phase width of the input beam was taken equal to 70 degrees. The energy histogram for the particles at the output of the accelerator is presented in Fig 4. The energy distribution of the particles is given taking into account the emission law. As one can see from the histogram the beam consists of two parts: $W < 0.17$ MeV and $W > 0.49$ MeV. The phase width of the accelerated part of the beam is not more than 50 degrees. Analysis of the data obtained shows that 80% of output particles have the

Fig. 1 General layout of accelerating section.



[9] C. Travier. Part. Accelerators. 1991, Vol. 36, pp.33-37

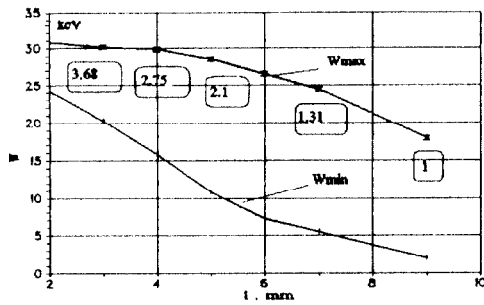


Fig. 2 Maximum and minimum energy as versus gap length (U=35 kV)

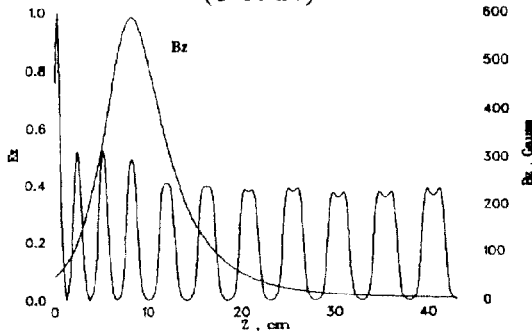


Fig. 3 Optimal distribution of the accelerating field and magnet field of the coil (for $I_b=0.078$ A) on the axis.

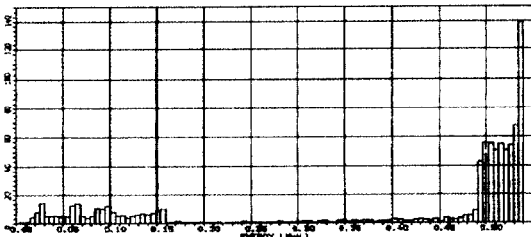


Fig. 4 The energy histogram for the particles at the output of the accelerator

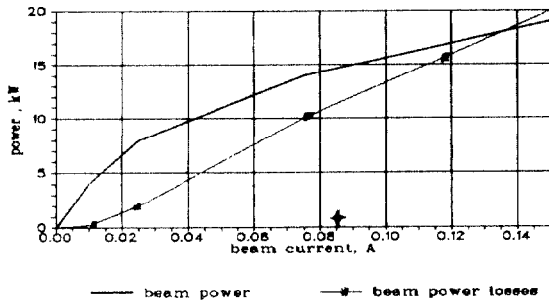


Fig. 5 Output beam power and beam power losses in the linac versus the beam current.

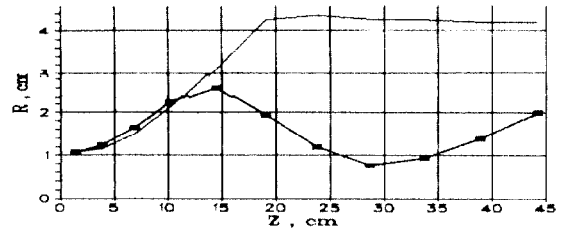


Fig. 6 The envelope of the beam (90%) along the linac without lens (—) and with focusing lens (—■—) at $I_b=0.078$ A.

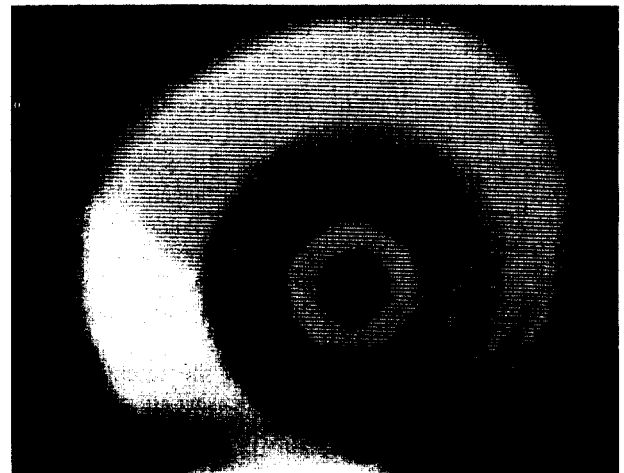
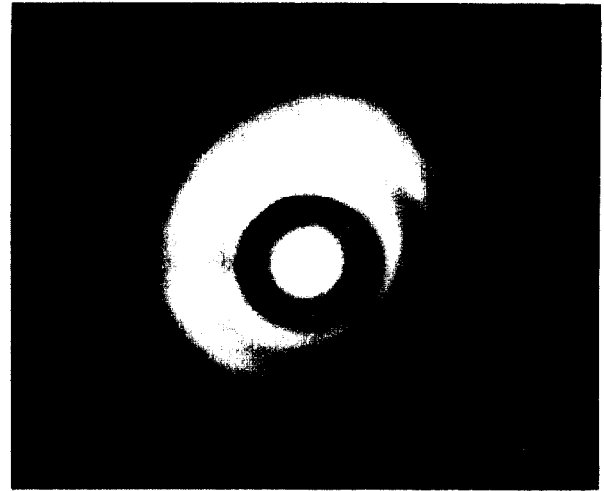


Fig. 7 a - photo of the drift tube of the structure with RF switched on and a cathode heating switched off;
b- photo of the drift tube of the structure with a cathode heating and RF power switched on.

energy more than 490 keV, radius of the beam (90%) and the divergence of the particles in the beam (90%) are not more than 3.05 mm and 5.1 mrad respectively. The results of the calculations show that the accelerated part of the beam is quite a formed bunch which can be used for further transportation and acceleration.

1.3. Estimation of the maximum beam current.

To estimate the maximum output current below the saturation level, Lengmure equation may be used :

$$I = 2.34 \times 10^{-6} S U^{3/2} / d^2 \quad , (A)$$

where S - surface of the cathode, cm²; d - distance between cathode and anode, cm; U - gap voltage, V.

The maximum current of accelerated fraction of the beam was calculated by code RTMTRACE, taking into account a time factor and dependence of the beam passing through the linac on the initial phase. Maximum value of the output current of the linac with RF gun appeared to be 78 mA. RF power dissipated in the accelerator was 16 kW.

1.4 Space charge effects

Space charge effects were calculated using the code PARMELA.

It is evident, that the number of particles passed through the linac decreases with increase of beam current. Fig.5 shows power losses of the beam in the linac versus the beam current. Supposing, that beam losses should be less than 10% of the whole RF power transferred into the beam, we can limit the region of operating currents for the accelerator. In this case, shown in Fig.5, allowed current is 0.015 A, output beam power is 6.7 kW. Thus, the accelerator enables to obtain beam currents up to 15 mA, using the klystron developed for the Moscow RTM project without any countermeasure for compensating space charge effects.

To produce the maximum beam current, as it follows from the results presented above, it is necessary to use focusing elements. A solenoidal coil above the accelerator structure is simple and effective for changing the focusing magnetic field. So, Fig.6 shows the behaviour the envelope of the beam (90%) along the linac without lens and with lens for the output beam current 0.078 A. The beam power losses for Ib=0.078 A with focusing lens are shown in Fig.5 by marker.

The maximum characteristics of the accelerator with RF gun without focusing and with focusing are as follows:

	with coil		
frequency	2450	2450	MHz
linac length	44.5	44.5	cm
RF power	22	53	kW
maximum energy	540	540	keV
maximum output beam current	12.5	78	mA
maximum beam power	6.2	34	kW
beam losses along linac	700	770	W

2. SECTION MANUFACTURING.

On the basis of the calculations, the construction of the accelerating section with RF gun was designed. The section consists of two parts : the first consists of three cells, including A cell with a cathode, and the second of 9 accelerating cells, including RF power input cell. Both parts were separately brased in hydrogen furnace and then bolted together at vacuum and RF seals.

After manufacturing the cells of the structure tuning of the cells frequencies and measurements of the field distribution on the accelerator axis has been carried out. As it was expected, experimental field distribution after first tuning iteration did not coincide with the required one. Consequent tuning iterations were made by changing the coupling between the neighbouring cells by means of increasing the angular dimensions of coupling slots. Experimental tuning of the structure was combined with the calculations by code CONTUR based on the coupled circuit model [7]. After several iterations of experimental tuning and corresponding calculations the experimental field distribution was matched with the calculated one (Fig.3). After brasing fine tuning of the cells frequencies was carried out with a help of special instruments.

Tuned section was investigated at high RF power level with the impregnated tungsten cathode. Preliminary experiments showed current instability from the cathode when the heater current was switched on. As a result the cathode melted at high levels of RF power. A similar effect was observed earlier at microtrons [8] and pulsed RF guns [9], and was explained by backward electron bombardment by the electrons which were not captured into acceleration. Our estimations show that the power dissipated at the cathode as a result of backward bombardment was about 12.5 W/mA, at the same time the nominal heating power of the impregnated tungsten cathode is 6 W only. A photo in Fig.7a shows the drift tube of the structure with RF switched on and a cathode heating switched off. A photo in Fig.7b shows the drift tube of the structure with a cathode heating and RF power switched on.

Presently we analyse a possibility of changing the impregnated tungsten cathode by a cathode of other type, and also model the methods of reduction of the intensity of backward electron current.

REFERENCES:

- [1] A.S.Alimov et al. NIM A326(1993), pp.391-398.
- [2] J.L.Warren, T.L.Buller, A.M.Vetter. Proc. of the 1989 IEEE PAC, pp.420-422.
- [3] A.G.Abramov et al., IHEP 83-3, Serpuchov(1983) preprint.(in RUSSIAN)
- [4] V.G.Gevorkyan et al. Deposited at VINITI No 183-B89(1989)(in RUSSIAN).
- [5] K.R.Crandal and L.Young, LANL rep. LAUR-90-1766(1990)57.
- [6] V.K.Grishin et al. NIM A255(1987), pp.431-436.
- [7] A.V.Tiunov, V.I.Schvedunov. Deposited at VINITI No.3319-B89(1989)(in RUSSIAN).
- [8] V.Melekhin. NIM A337(1993), pp.29-33